Self-Assembled Nanotapes of Oligo(*p*-phenylene vinylene)s: Sol–Gel-Controlled Optical Properties in Fluorescent π-Electronic Gels

Subi J. George and Ayyappanpillai Ajayaghosh*[a]

Abstract: A rational approach to the design of supramolecular organogels of all-*trans* oligo(*p*-phenylene vinylene) (OPV) derivatives, a class of well-known organic semiconductor precursors, is reported. Self-assembly of these molecules induced gelation of hydrocarbon solvents at low concentrations (<1 mM), resulting in high aspect ratio nanostructures. Electron microscopy and atomic force microscopy (AFM) studies revealed twisted and entangled supramolecular tapes of an average of 50–200 nm in width, 12–20 nm in thickness, and several micrometers in length. The hierarchical growth of the entangled tapes and the consequent gelation is attributed to the lamellar-type packing of the molecules, facilitated by cooperative hydrogen bonding, π stacking, and van der Waals interactions between the OPV units. Gelation of OPVs induced remarkable changes in the absorption and emission properties, which indicated strong electronic interaction in the aggregated chromophores. Comparison of the absorption and emission spectra in the gel form and in the solid film indicated a similar chromophore organization in both phases. The presence of self-assembled aggregates of OPVs was confirmed by solvent- and temperature-dependent changes in the absorption and emission properties, and by selective excitation experiments. This is the first detailed report of the gelation-induced formation of OPV nanotapes, assisted by weak, nondirectional hydrogen-bonding motifs and π–π stacking. These findings may provide opportunities for the design of a new class of functional soft materials and nanoarchitectures, based on π-conjugated organic semiconductor-type molecules, thereby enabling the manipulation of their optical properties.

Keywords: nanostructures · oligo(*p*-phenylene vinylene)s · organogels · self-assembly · supramolecular chemistry

Introduction

The control of the self-assembly of synthetic molecules in the creation of nanosized architectures, using the principles of supramolecular chemistry, is a topic of considerable importance.[1] The cooperative effect of noncovalent forces, such as hydrogen bonding, π stacking, dipolar and van der Waals interactions, is the driving force behind molecular self-assembly, leading to a variety of novel supramolecular architectures with reversible functional properties. Nature can control the architecture and function of supramolecular assemblies, such as the DNA double helix, the collagen triple helix, ion channels, and photosynthetic reaction centers, and this has been the major source of inspiration for scientists to mimic natural systems with the help of synthetic molecules.[2–6] In the domain of functional molecular assemblies and nanoarchitectures, the supramolecular control of chromophore-linked molecular systems is a challenge, particularly in the fabrication of nanoscale devices, as chromophore orientation has tremendous influence on optoelectronic properties.[7] Because organic π-conjugated systems play a crucial role in supramolecular devices due to their interesting optical and electronic properties, the modulation of their optical properties by intermolecular interactions is of great significance.[3,8] In this context, the supramolecular chemistry of phenylene vinylenes has attracted considerable attention and is the focus of much research.[9]

An interesting feature of the noncovalent interactions in certain organic molecules is their ability to entrap large vol-

[a] S. J. George, Dr. A. Ajayaghosh
Photosciences and Photonics Division
Regional Research Laboratory, Trivandrum 695019 (India)
Fax: (+91) 471-251-5306
E-mail: aajayaghosh@rediffmail.com

Supporting information for this article is available on the WWW under http://www.chemeurj.org/ or from the author: General experimental procedures, synthesis, and characterization data of OPVs, binary phase diagrams obtained by plotting T_{gel} vs. concentration, DSC thermograms, OPM picture of **OPV1a** and SEM pictures of **OPV5** and **OPV7** self-assemblies, time-resolved fluorescence decay profiles of **OPV1a**, and a table containing photophysical properties of the OPVs under investigation.

 DOI: 10.1002/chem.200401178

umes of solvents within the supramolecular nano- and mesoscopic structures to form gels in appropriate solvents.[10] The properties exhibited by this novel class of supramolecular materials, with respect to the reversible self-assembly phenomena, are striking in comparison to those exhibited by the polymer-based organogels formed by permanent covalent interactions.[11] The recent and rapid growth in interest in small-molecule-based organogelators is due to several potential applications ranging from cosmetics, catalysis, and controlled release to optoelectronics and related fields. Several organic molecules are known to form organogels with the help of hydrogen bonding, π stacking, dipole–dipole or van der Waals interactions.[12–17] However, chromophore-based organogelators,[18] particularly gels based on extended π-conjugated systems,[19] are relatively few. Although the self-assembly of oligo(*p*-phenylene vinylene)s (OPVs) is fairly well understood, the design of supramolecular nanoarchitectures and their properties was not elucidated until our preliminary studies on OPV gels.[20] Here, we describe details of the self-assembly of OPVs into supramolecular nanotapes of high aspect ratio, and the consequent gelation behavior that leads to the remarkable modulation of optical properties.[21]

Results and Discussion

Design strategy: The bottom-up creation of three-dimensional organic nanoarchitectures on the one hand, and gelation on the other hand, is a delicate balance between the crystallization, precipitation, and solubility of noncovalently interacting molecules in a suitable solvent. With this in mind, a variety of tailor-made OPV derivatives were synthesized, the structures of which are represented in Figure 1. These molecules have many features that facilitate the formation of a three-dimensional self-assembly, as depicted in Figure 2a. The presence of the two hydroxymethyl end-groups allows the molecules to self-assemble by weak, non-directional 2-point hydrogen bonding, and the long hydro-

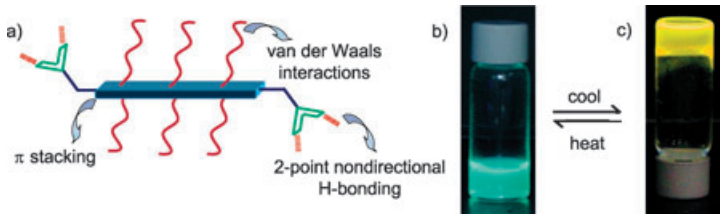

Figure 2. a) Design features of OPVs. b) and c) **OPV1a** in decane under illumination before and after gelation, respectively.

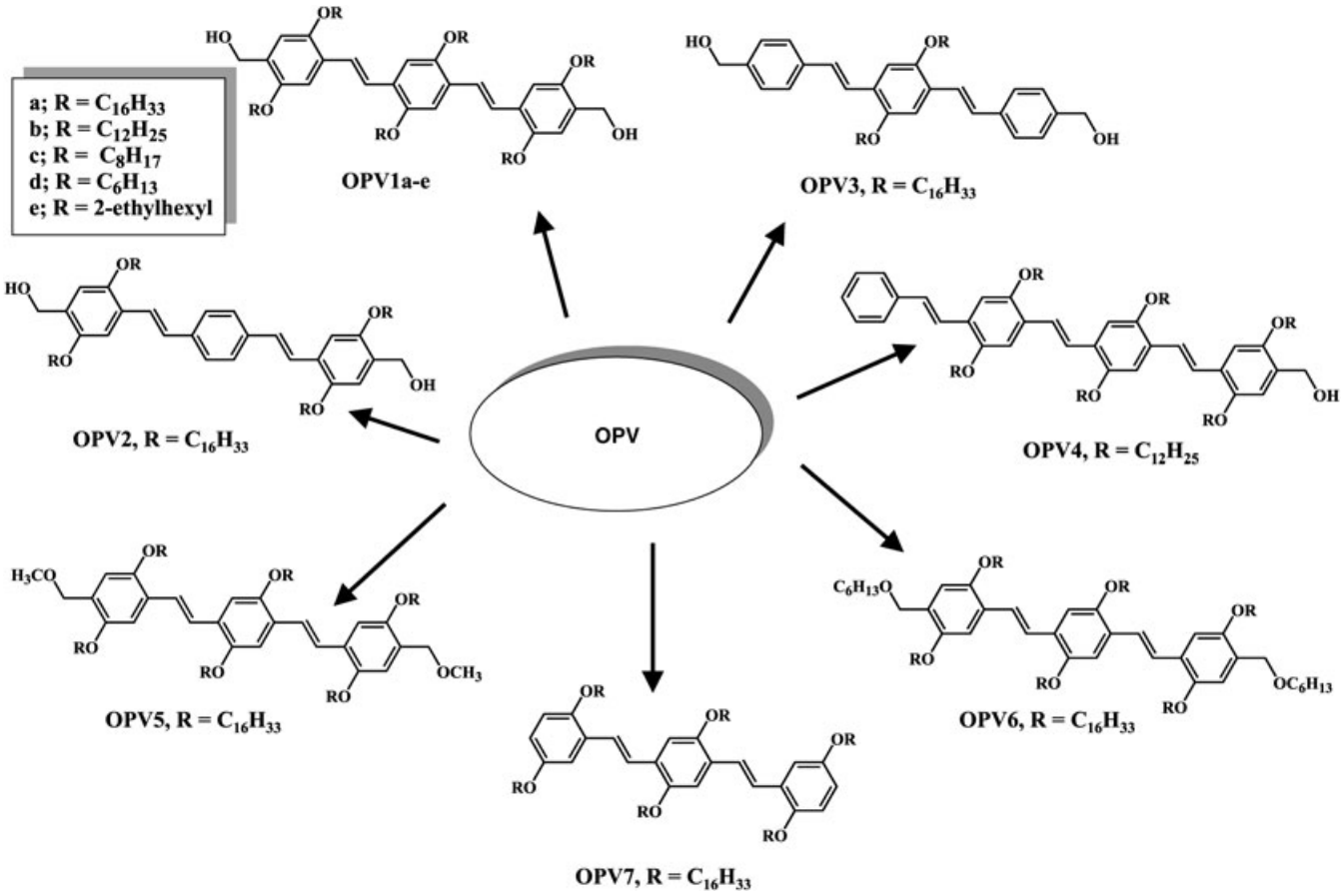

Figure 1. Library of the OPV derivatives under investigation.

carbon side-chains control the balance between solubility and crystallization, as well as the packing of the molecules. The rigid aromatic OPV backbone facilitates the π–π stacking of the molecules. Cooperative interactions of these noncovalent forces eventually lead to the formation of entangled nanoscopic structures, which are able to hold a large amount of the appropriate solvent molecules within the self-assembly, thereby forming a gel.

Synthesis of OPVs: The bisalcohols **OPV1a–e**, **OPV2**, and **OPV3** were synthesized by means of the controlled Wittig reaction of the appropriate bisaldehydes and bisphosphonium salts, followed by reduction of the resulting OPV bisaldehydes with $NaBH_4$ (Scheme 1).[22] The controlled Wittig–Horner reaction between the bisaldehyde (**1**) and the benzyl phosphonate (**2**) afforded the monoaldehyde **3** in 35% yield, which in turn was reduced to **OPV4** by $NaBH_4$ in 95% yield (Scheme 1). Synthesis of **OPV7** was based on a published procedure (90% yield).[23] Preparation of the hydroxyl-protected derivatives **OPV5** and **OPV6** was accomplished by the alkylation of **OPV1a** with the corresponding alkyl halides in 95% and 60% yields, respectively (Scheme 2). All OPV derivatives under investigation were characterized by spectral analyses. The all-*trans* configurations of the OPVs were confirmed by the *J* values (16.5 Hz) of the vinylic protons in their respective ^1H NMR spectra.

Self-assembly and gelation: The dissolution of small amounts of the newly synthesized OPV derivatives in a specific volume (1 mL) of different solvents, under heating and cooling, resulted in the spontaneous gelation of the solvents, indicating the formation of extended self-assemblies. The gels obtained were transparent and stable, so that the glass vial could be turned upside down without damaging the structure (Figure 2c). Illumination of the OPV solutions before gelation revealed strong greenish-blue fluorescence, which changed upon gelation to greenish-yellow emission (Figure 2b and c). The results of the gelation experiments are presented in Table 1 and reveal that the bishydroxy compounds **OPV1a–c**, which have long, linear hydrocarbon chains, are efficient gelators of nonpolar hydrocarbon solvents, such as hexane, decane, dodecane, cyclohexane, benzene, and toluene. The critical gelator concentrations (CGC) of **OPV1a** in dodecane, decane, and cyclohexane were 0.8,

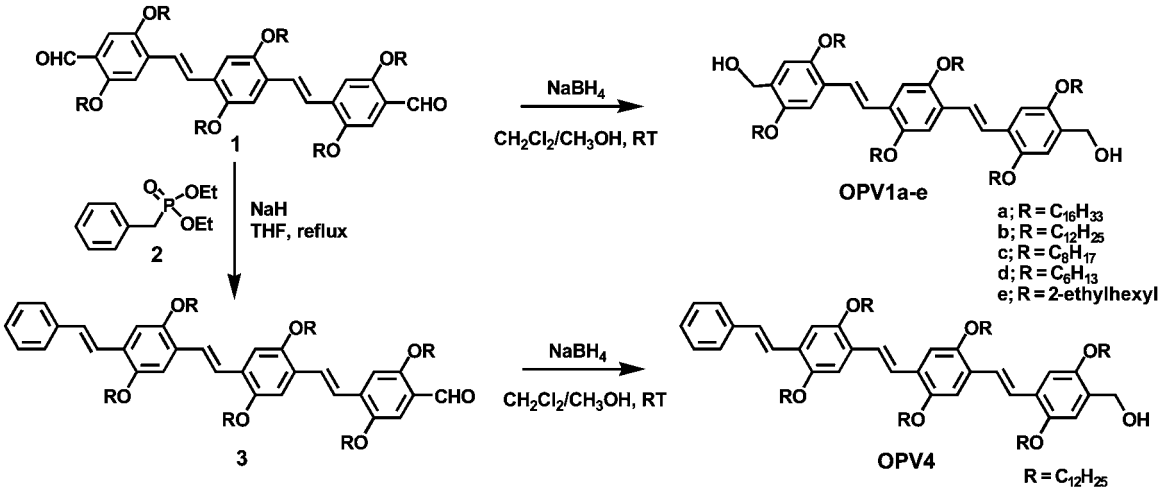

Scheme 1. Synthesis of mono- and bishydroxy OPV derivatives.

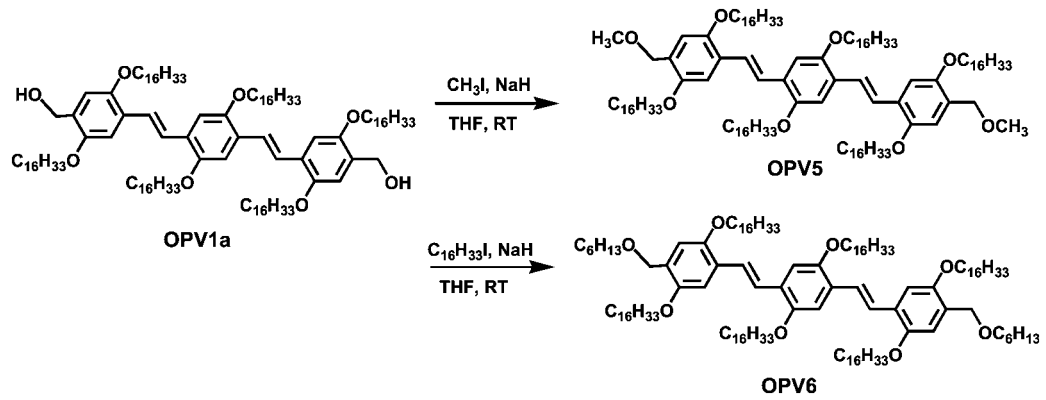

Scheme 2. Synthesis of the hydroxyl-protected OPVs, **OPV5–6**.

Table 1. Critical gelator concentrations (CGC)[a] [mM] of **OPV1a–e**, **OPV2**, and **OPV3** in different solvents.

Gelator	Dodecane	Decane	Cyclohexane	Hexane	Toluene	Benzene	Chloroform
OPV1a	0.8 (s, tr)	0.9 (s, tr)	1.1 (s, tr)	1.7 (s, tr)	2.8 (s, tr)	3.0 (s, tr)	5.6 (th, o)
OPV1b	1.0 (s, tr)	1.1 (s, tr)	1.4 (s, tr)	2.1 (s, tr)	4.2 (s, tr)	4.1 (s, tr)	17.3 (th, o)
OPV1c	4.5 (PG)	4.8 (PG)	6.3 (s, tr)	I	12.6 (s, tr)	11.6 (s, tr)	S
OPV1d	I	I	10.6 (s, tr)	I	15.9 (s, tr)	16.0 (s, tr)	S
OPV1e	S	S	S	S	S	S	S
OPV2	PS	PS	15.4 (s, o)	11.5 (s, o)	23.0 (s, o)	PS	PS
OPV3	PS	PS	PS	I	PS	PS	S

[a] CGC is the minimum concentration required for the formation of a stable gel at room temperature. In parenthesis; s = stable, tr = transparent, th = thixotropic, o = opaque. S = soluble ($>25\ mg\,mL^{-1}$), I = insoluble, PS = poor solubility, PG = partial gelation at room temperature.

0.9, and 1.1 mM, respectively. This means that **OPV1a** can entrap approximately 10000 molecules of dodecane per gelator molecule and can be considered a supergelator.[24]

The gelation ability of **OPV1d**, which carries hexyloxy side chains, is relatively poor (the CGC is 10 mM in cyclohexane), whereas **OPV1e**, which has branched 2-ethylhexyloxy side chains, gave a homogeneous solution in all of the solvents investigated. The nature of the solvents has considerable influence on the gelation behavior of **OPV1a–d** (Table 1). For example, the CGC of **OPV1a** in chloroform is 5.6 mM and the gel formed is unstable upon shaking (thixotropic). However, in toluene, **OPV1a** forms a reasonably stable gel with a CGC of 2.8 mM. The number of the hydrocarbon side chains present on the conjugated backbone significantly influences gelation behavior (Table 1). For example, the CGC of **OPV2** in cyclohexane is 15.6 mM resulting in a turbid gel, whereas **OPV3** does not gelate any of the solvents investigated.

To investigate the role of hydrogen-bond-assisted π stacking in the gelation process, we extended our studies to other OPV derivatives (**OPV4–7**). The results are summarized in Table 2. Interestingly, in the case of **OPV5** and **OPV6**, gelation occurred only at high concentrations, compared to the case of **OPV1a**. The CGC of **OPV5** is 3.3 mM in cyclohexane and the resultant gel is thixotropic, which may be due to the absence of hydrogen-bond donor groups that are necessary for the positional locking of the molecules within the π-stacked assembly. Compound **OPV6**, with the hexyloxy end-groups, could gelate solvents such as dodecane and decane only at high concentrations. In the case of **OPV4** with one terminal hydroxymethyl group, gel formation was observed in nonpolar solvents, though it was not as efficient as in the case of **OPV1a** and **OPV1b**. However, **OPV7**, without any functional end-groups, could not gelate any of the solvents investigated. Instead, aggregate formation was observed above a concentration of 1×10^{-5} M, as indicated by the shoulder absorption band at 470 nm in dodecane, but no solvent molecules could be trapped. These studies indicate that an optimum balance of hydrogen bonding, π stacking, and van der Waals interactions is crucial in the process of self-assembly and gelation.

Table 2. Critical gelator concentrations [mM] of **OPV4–7** in different solvents.[a]

Gelator	Dodecane	Decane	Cyclohexane	Hexane	Toluene	Benzene	Chloroform
OPV4	1.4 (s, tr)	1.5 (s, tr)	2.3 (s, tr)	4.6 (th, o)	4.6 (s, tr)	4.2 (s, tr)	S
OPV5	1.6 (th, tr)	1.8 (th, tr)	3.3 (th, tr)	4.4 (th, tr)	7.2 (th, tr)	6.8 (th, tr)	16.5 PG
OPV6	4.9 (th, tr)	5.2 (th, tr)	10.4 (th, o)	10.4 (th, o)	S	S	S
OPV7	PS	PS	PS	PS	PS	PS	PS

[a] In parenthesis; s = stable, tr = transparent, th = thixotropic, o = opaque. S = soluble ($>25\ mg\,mL^{-1}$), PS = poor solubility, PG = partial gelation at room temperature.

Thermotropic behavior: The thermotropic behavior of the gels formed by **OPV1a–c** and **OPV4–7** was investigated by using the dropping ball method and differential scanning calorimetry (DSC) to study the impact of the structure of the OPVs and the nature of the solvents on gel stability (see Supporting Information). In the case of **OPV1a–c**, a regular increase in the melting temperature of the gel (T_{gel}) was observed as the concentration of the gelator molecules increased. The increase in T_{gel} that accompanied an increase in alkyl chain length demonstrates the enhanced stability of the gels, which could be due to the solvation-assisted intermolecular packing of the long alkyl chains. Phase diagrams of **OPV1a** gels from dodecane, cyclohexane, toluene, and chloroform revealed that **OPV1a** forms strong gels in dodecane and cyclohexane, even at very low concentrations. This observation is in accordance with the gelation studies presented in Table 1. A comparison of the phase diagrams of the cyclohexane gels of **OPV1a**, **OPV4**, and **OPV5** at different concentrations revealed remarkable stability of the **OPV1a** gel, due to hydrogen bonding between the hydroxymethyl groups. For example, a cyclohexane gel of the methoxy derivative **OPV5** ($10\ mg\,mL^{-1}$) melts at 47 °C, which is 15 °C lower than the melting temperature of the corresponding **OPV1a** gel. Clearly, the gel of the monohydroxy derivative **OPV4** is more stable than that of the hydroxyl-protected **OPV5** gel, although less stable than the **OPV1a** gel.

In the cases of **OPV1a–c**, the transition temperatures of the heating exotherms and cooling endotherms increase in the order **OPV1a** > **OPV1b** >

OPV1c. In agreement with the dropping ball experiment, DSC analysis confirmed increased stability of the gels in hydrocarbon solvents of greater chain length. The role of hydrogen bonding is also evident from the DSC thermograms, in which **OPV1a** exhibited a melting temperature of 63.5 °C, which is 12.5 °C and 14 °C higher than that of **OPV4** and **OPV5**, respectively.

Variable temperature ^{1}H NMR spectroscopy studies: The ^{1}H NMR spectra recorded at room temperature of **OPV1a–b** in $CDCl_3$ or [D_6]benzene displayed distinctly solvent-dependent features. For example, the ^{1}H NMR spectrum of **OPV1a** in $CDCl_3$ (up to 4 mM) showed well-resolved resonance signals in agreement with the structure of the molecule, whereas in [D_6]benzene (5 mM), none of the characteristic resonance signals corresponding to the aromatic and vinylic protons was seen. These observations indicate strong intermolecular interactions due to the aggregation of the OPV units in [D_6]benzene. In such cases, the long correlation time produces ^{1}H NMR signals that are too broad and weak to be distinguished. Changes in the resonance signals of the aromatic and vinylic protons obtained within the temperature range of 10–70 °C are shown in Figure 3a. As the

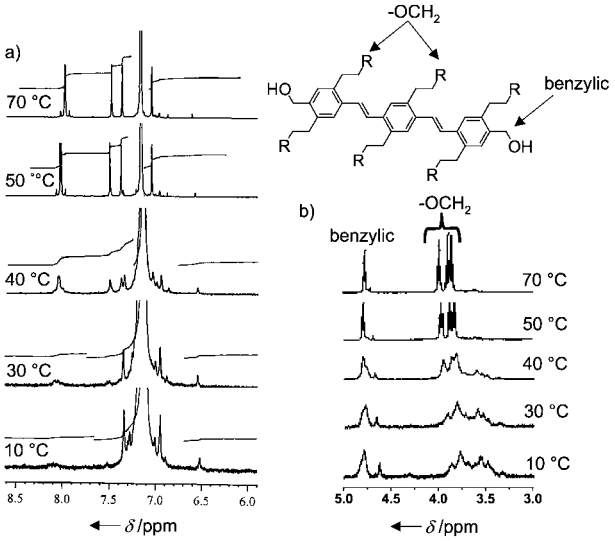

Figure 3. Temperature-dependent ^{1}H NMR spectra of **OPV1a** in [D_6]benzene (5 mM); a) for the aromatic and vinylic protons, b) for the aliphatic protons.

temperature increases, the resonance signals corresponding to the aromatic protons appeared gradually at $\delta = 7.49$, 7.37, and 7.05 ppm, along with the vinylic protons at $\delta =$ 8.05 ppm. The corresponding changes to the aliphatic protons can be seen in Figure 3b. The benzylic and $-OCH_2$ protons, which appeared as broad, unresolved peaks at $\delta = 4.79$ and 3.65–3.9 ppm, respectively, became well resolved when the temperature was increased to 50 °C. Further heating produced no significant change, except for a small, upfield shift of vinylic protons from 8.05 to 7.95 ppm.

Microscopy: The results of optical polarizing microscopy of the OPV gels indicated the formation of strongly birefringent textures, characteristic of the mesoscopic alignment of the chromophores during gelation (see Supporting Information). Scanning electron microscopy (SEM) images of the dried **OPV1a** gels from toluene and decane revealed entangled networks of twisted supramolecular tapes formed by the self-assembly (Figure 4a and b). Careful analysis re-

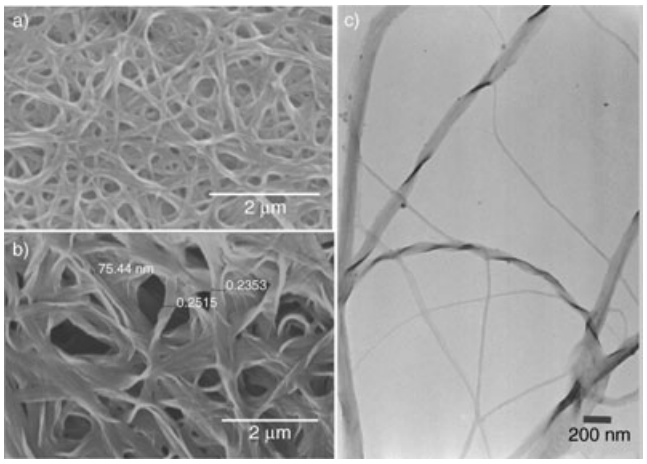

Figure 4. SEM images of **OPV1a** from a) toluene and b) decane. c) TEM image of the **OPV1a** gel from toluene. Samples for TEM images were prepared by drop casting the OPV solution from toluene or decane on carbon-coated copper grids. The pictures were obtained without staining.

vealed that the twisted tapes of the toluene gel are approximately 50–100 nm in width and several micrometers in length. However, in the case of the decane gel, the fibers are more dense, entangled, and twisted. The relatively large size of the gel structures in this case indicates that the interactions between individual tapes in decane are much stronger than those in toluene, thereby leading to the formation of large, twisted tapes. Thus, the gelation efficiency and the stability of the OPV gels are in agreement with the observed morphology. The difference in the gelation behaviors of **OPV1a**, **OPV5**, and **OPV7**, which is attributed to the effect of the hydrogen-bonding group in the hierarchical growth of the self-assembly, is clear from the different morphologies observed by SEM analysis (see Supporting Information). The transmission electron micrograph (TEM) of **OPV1a** from a dilute toluene solution provides more information on the morphology of the self-assembled textures (Figure 4c), and shows the presence of isolated and randomly twisted tapes of 50–100 nm in diameter and several micrometers in length. Both right- and left-handed twists are visible. The presence of several thin fibers of 10–20 nm in diameter could also be seen in addition to the large, twisted structures.

The atomic force microscopy (AFM) image of the **OPV1a** gel in toluene (Figure 5) is in full support of the tape-like morphology of the self-assembly, as observed by SEM and TEM analyses. It is also clear that the fiber bun-

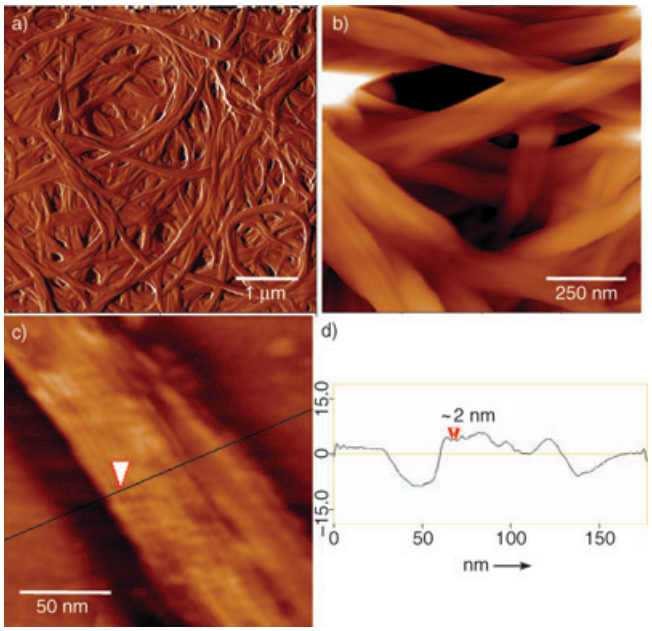

Figure 5. AFM images displaying the a) amplitude and b) height of **OPV1a** from toluene under different magnifications. c) Image of an isolated **OPV1a** gel fiber and d) a cross-sectional profile of the supramolecular tape displayed in (c). Samples were prepared by drop casting the OPV solution onto a freshly cleaved, muscovite mica surface.

dles observed in the AFM images are built up from thinner fibers of 10–20 nm in width. The width of the smallest fiber bundle that can be distinguished is 50–70 nm. Several isolated fibers could be observed by AFM, whereby a dilute solution of **OPV1a** was deposited by drop casting. The morphology of such a single fiber is shown in Figure 5c. The array of dark and bright areas of approximately 2 nm in width, as seen in the cross-sectional profile of the **OPV1a** fiber in Figure 5d, indicate the lamellar organization of the individual OPV units at the molecular level. The detailed cross-sectional analysis revealed that the thickness of the tapes, which are several micrometers in length, is in the range 12–20 nm and the widths are 50–200 nm. Notably, the large width and thickness of the tapes is an indication of the three-dimensional growth of the self-assembly, in contrast to the formation of one-dimensional assemblies of other reported systems.[21]

X-ray diffraction studies: The xerogels obtained from **OPV1b** exhibited well-resolved X-ray diffraction patterns that were characteristic of the long-range ordering of the molecules (see Supporting Information). A strong diffraction signal corresponding to a d-spacing of 23.2 Å, which is close to the calculated molecular length (21.2 Å) of **OPV1b**, could be seen, along with several higher-order reflection peaks in the small-angle region. A prominent reflection characteristic of a typical π–π stacking distance was observed in the wide-angle region at 3.8 Å. The intense diffraction peaks of **OPV1a**, **b**, and **d** at the short-angle region corresponded to d-spacings of 41.7 Å, 35.2 Å, and 16.5 Å, respectively. These distances match the calculated width of the respective molecules with extended side chains and indicate the lamellar packing distances, which should vary with the length of the side chains, as seen by comparison of the observed d-spacing (Supporting Information). Based on this data, it appears that the xerogel of **OPV1b** is formed by lamellar-type packing through hydrogen bonding, π stacking, and van der Waals interactions, as shown in Figure 6. In the lamellar packing, **OPV1b** adopts a planar structure, in which the aryl units are coplanar and the alkyl side chains are laterally extended, with a complete stretching of the side chains within the same plane as the conjugated backbone. The diffraction patterns of **OPV5** carrying hexadecyl side

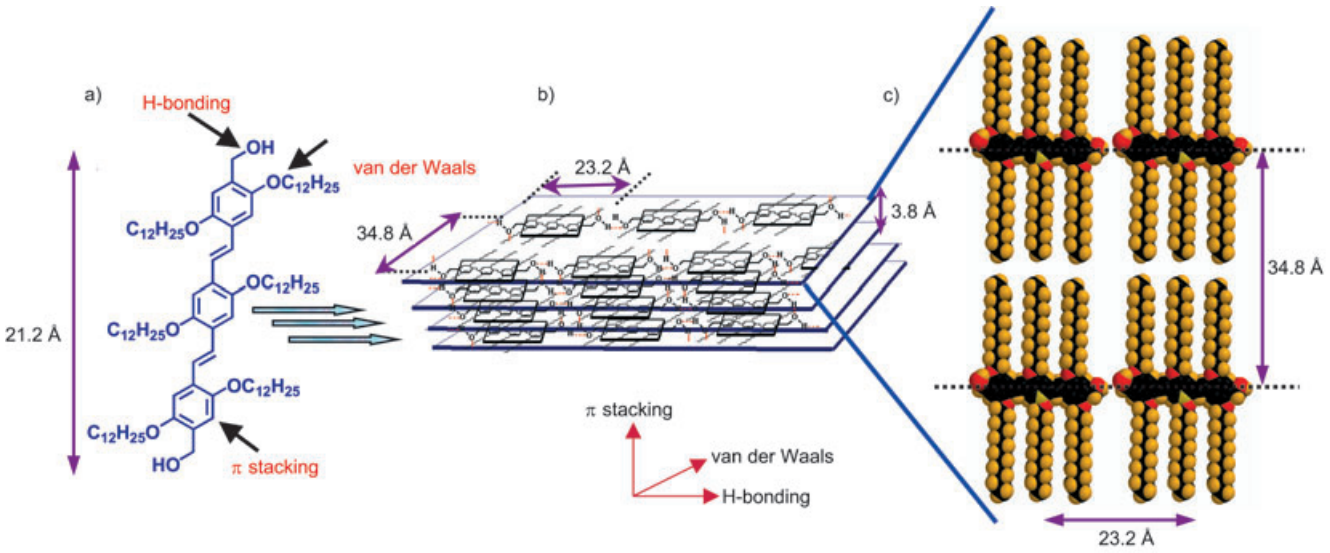

Figure 6. Schematic view of the lamellar packing of **OPV1b** in the gel state. a) Structure of **OPV1b**, b) side view of the lamellar packing, and c) top view of the molecular model.

chains, in which the hydrogen bonding of the two hydroxymethyl groups was blocked, displayed relatively broad reflections. The absence of higher-order reflections and the presence of broad reflections in the wide-angle region suggest a low degree of ordering in this case. This data is in agreement with the gelation behavior of **OPV1a** and **OPV5**, as indicated in Tables 1 and 2.

Based on the results obtained by ^{1}H NMR spectroscopy, X-ray diffraction, and microscopy, it is clear that the supramolecular tapes of the OPV units, formed by the cooperative hydrogen bonding, π stacking, and van der Waals interactions, are responsible for gelation. The weak, nondirectional hydrogen-bonding interaction of the hydroxymethyl end-groups enables the formation of linear, hydrogen-bonded assemblies (Figure 6), which form supramolecular layers by lamellar packing. The layered assemblies are reinforced by π stacking and van der Waals interactions, leading to the formation of three-dimensional, supramolecular tapes. Hydrogen bonding may also facilitate the reversible, noncovalent cross-linking between layers to produce a network assembly. The extended growth of these assemblies results in twisting of the tapes to form elongated networks. This facilitates the immobilization of large volumes of solvents within and between the networks, resulting in gelation.

Self-assembly-induced modulation of optical properties: The most important feature of the gelation of OPVs is the alteration observed in the optical and photophysical properties (see Supporting Information). The absorption and emission spectra of **OPV1a** under different experimental conditions are represented in Figure 7a and b. In chloroform (1×10^{-5} M) the absorption maximum of **OPV1a** is observed at 407 nm. In cyclohexane ($\lambda_{max}=401$ nm) and dodecane ($\lambda_{max}=404$ nm) the absorption maxima are slightly blue-shifted and the intensity of the π–π* band is decreased, with the formation of a red-shifted shoulder band at 467 nm. Upon heating the same solutions to 65 °C, the shoulder band at 467 nm disappeared and the original intensity of the π–π* transition was regained, as in the case of chloroform, except for a slight red-shift of the absorption maxima. This latter effect could be due to the change in the solvent polarity. Interestingly, the absorption spectrum of a film of **OPV1a** closely resembled the spectrum corresponding to the dodecane solution. In chloroform, **OPV1a** showed an intense blue emission with maxima of around 463 and 490 nm ($\Phi_f=0.73$), whereas in dodecane the emission was completely shifted towards the long-wavelength region (green emission), with maxima of around 537 and 567 nm. However, in cyclohexane at room temperature, a broad emission with several maxima at 454, 476, 527, and 561 nm ($\Phi_f=0.28$) was obtained, the relative intensities of which are dependent upon temperature and concentration (Figure 7b). As the concentration increases, the solution becomes gel-like and the emission changes to greenish-yellow, probably due to the scattering of light (Figure 2c). Upon heating the cyclohexane or dodecane solution, the emission changes to blue and the

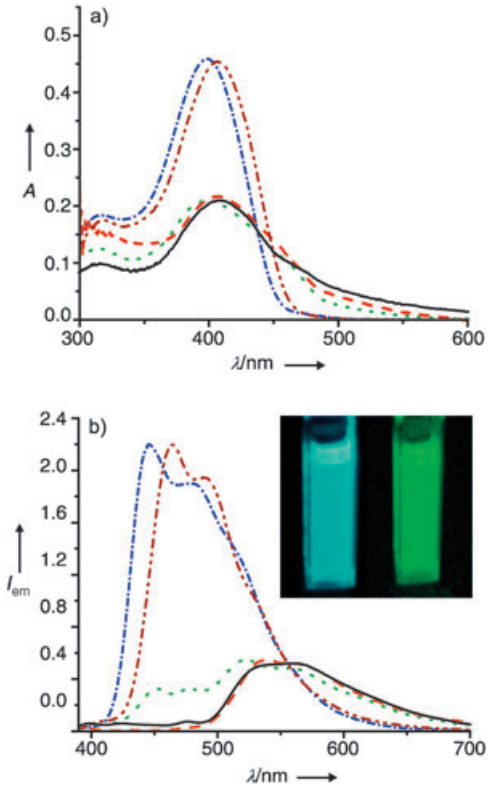

Figure 7. Absorption (a) and emission (b) spectra of **OPV1a** (1×10^{-5} M) in chloroform (–··–··–), cyclohexane (•••••), dodecane at 25 °C (——), dodecane at 65 °C (–•–•), and in the solid state (– – –) as a coated film ($\lambda_{ex}=$ 380 nm). Inset shows the temperature-dependent visual change in the emission colors of the molecularly dissolved (left) and self-assembled (right) molecules in dodecane.

spectrum matches that in chloroform, except for a slight red-shift. The thermoreversible visual color change in the emission of **OPV1a** in dodecane is shown in the inset of Figure 7b. Similar to the absorption changes, the emission of the **OPV1a** film corresponded to that in dodecane. These observations reveal that in chloroform, **OPV1a** prefers to be in the molecularly dissolved, monomeric form, whereas in dodecane or in film form, it exists as a self-assembled species. However, in cyclohexane at room temperature, **OPV1a** molecules are present in more than one co-existing species, the composition of which varies as a function of concentration and temperature. The resemblance of the absorption and emission spectra of the **OPV1a** gel in dodecane at 25 °C with those of the drop-cast film indicates that the chromophore packing in the two cases is nearly identical.

Variable temperature UV/Vis and fluorescence spectra of **OPV1a** in dodecane revealed a transition, as the temperature was increased from 15 to 65 °C, from the self-assembled species to the molecularly dissolved species (Figure 8). In the UV/Vis spectra, an increase in the intensity of the absorption maximum at 404 nm was observed upon increasing the temperature. This is accompanied by a concomitant decrease in the intensity of the shoulder band at 467 nm through an isosbestic point at 428 nm (Figure 8a). Similarly, in the fluorescence spectra ($\lambda_{ex}=380$ nm) recorded as the

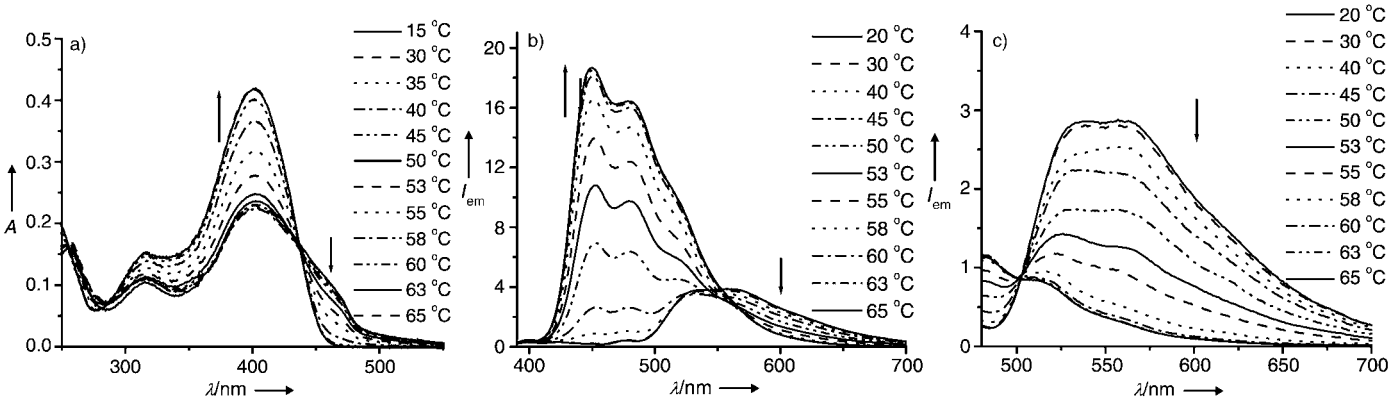

Figure 8. Temperature-dependent absorption and emission changes of **OPV1a** in dodecane (1×10^{-5} M). a) Absorption, b) emission on excitation at $\lambda_{ex}=$ 380 nm, and c) emission on excitation at $\lambda_{ex}=470$ nm.

temperature is increased from 20–65 °C, the intensity of the long-wavelength maxima at 537 and 567 nm decreases with the simultaneous increase in intensity of the emission bands at 452 nm and 459 nm (Figure 8b). These observations indicate the existence of self-assembled species at room temperature and nonassembled species at elevated temperatures. The gradual decrease in emission from the self-assembled species as the temperature was increased could be observed more clearly if the species were selectively excited at 470 nm (Figure 8b and c).

The temperature- and concentration-dependent shifts in the absorption and emission spectra are attributed to the self-assembled species and not to the formation of excimers. This is clear from the excitation and emission spectra of **OPV1a** in dodecane and cyclohexane (Figure 9). The first argument against excimer formation is the solvent- and temperature-dependent growth of the long-wavelength absorption shoulder in the UV/Vis spectrum, indicating ground-state interactions between molecules. Secondly, the excitation spectrum of **OPV1a** in dodecane at room temperature (monitored at 520 nm) matched the absorption spectrum having a maximum at 400 nm with a shoulder at 470 nm (Figure 9a). Interestingly, the excitation spectrum (dashed line) at higher temperatures (monitored at 520 nm) in dodecane did not show the shoulder band at 470 nm and matched the absorption spectrum. In addition, the excitation spectra of **OPV1a** collected at 450 and 620 nm matched the absorption spectra of the free and self-assembled **OPV1a** molecules, respectively (inset of Figure 9a). The presence of the self-assembled molecules is also justified by the formation of a red-shifted emission spectrum ($\lambda_{em}=527$ and 561 nm) of **OPV1a** in cyclohexane, following the selective excitation at the shoulder band of 470 nm, in contrast to the broad spectrum observed on excitation at 380 nm (Figure 9b). The time-resolved fluorescence analysis of **OPV1a** in chloroform revealed monoexponential decay with an excited state lifetime of 1.64 ns (100 %) at room temperature, whereas in cyclohexane, biexponential decay with lifetimes of 2.09 (57.85 %) and 0.82 ns (42.2 %) was obtained (see Supporting Information). In cyclohexane at 50 °C, monoexponential decay with a lifetime of 1.58 ns was observed, irrespective of the monitoring wavelength. These studies support the strong aggregation of OPVs in nonpolar solvents, which is concentration-, polarity-, and temperature-dependent. Notably, the extent of the aggregation-induced changes in the optical properties of **OPV1a–e** differs from observations in previous reports of hydrogen-bonded OPVs,[9b–e] indicating that the electronic interaction between the OPV

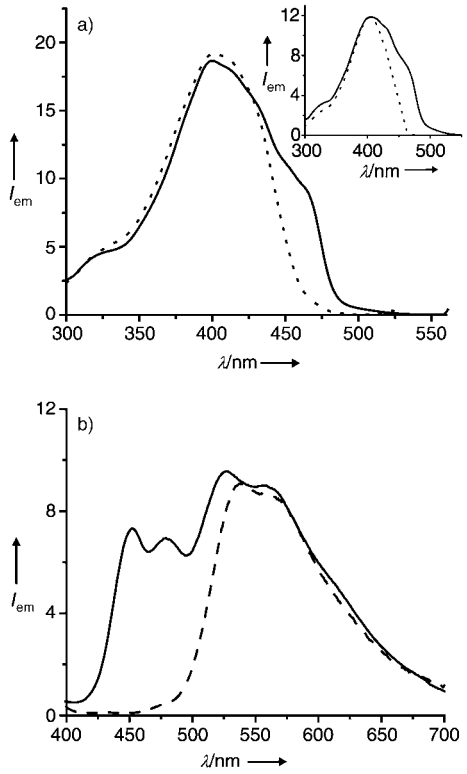

Figure 9. a) Excitation spectra ($\lambda_{em}=520$ nm) of **OPV1a** (1×10^{-5} M) in dodecane at 20 °C (——) and at 60 °C (•••••). Inset shows the excitation spectra in cyclohexane, collected at 450 (•••••) and 620 nm (——). b) Emission spectra of **OPV1a** in cyclohexane at an excitation wavelength of 380 (——) and 470 nm (– – –).

units in the present case is much stronger, leading eventually to gel formation.

The stability of the OPV self-assembly and the resultant gel under different experimental conditions could be determined from plots of aggregate fraction (α) against temperature, which are obtained by monitoring the temperature-dependent changes in the UV/Vis absorption spectra at 470 nm (Figure 10). As expected, the transition temperature of the **OPV1a** self-assembly increases upon changing the solvent from toluene to cyclohexane to dodecane (Figure 10a). The stability of the self-assembled molecules increases by 10–15 °C with each order of magnitude increase in concentration (Figure 10b). These stability responses obtained from the sigmoidal temperature transition curves of the OPV self-assembly are characteristic of the cooperativity of the different noncovalent interactions during the self-assembly process. Figure 10c reveals that the stability of the self-assemblies increases as the length of the alkyl chains increases, with a maximum stability exhibited by **OPV1a** with hexadecyl chains. Thus, the change in absorption and emission properties associated with the self-assembly is a useful tool to probe the sol–gel phenomena of OPVs. The efficiency of aggregation and the stability of the aggregates of OPVs, as determined by the change in optical properties, are in agreement with their gelation behavior, as shown in Tables 1 and 2.

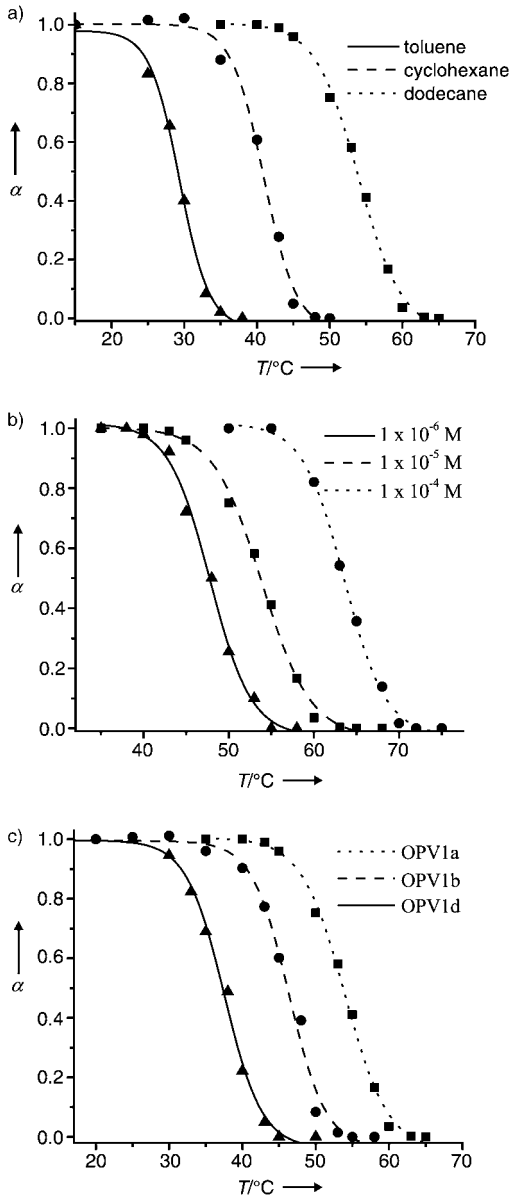

Figure 10. Stability of the OPV self-assemblies obtained from plots of aggregate fraction (α) versus temperature. a) **OPV1a** in different solvents, b) **OPV1a** at different concentrations, and c) **OPV1a**, **b**, and **d** in dodecane (1×10^{-5} M). The data points were obtained from the variable temperature absorption spectral changes at 470 nm.

Conclusion

We have illustrated a rational approach to the design of supramolecular nanotapes of OPVs that form a novel class of fluorescent organogels. Interestingly, although the OPVs described here are functionalized by one of the weakest, nondirectional hydrogen-bonding motifs, they form strong organogels when tailored with long hydrocarbon side chains. Detailed morphological studies revealed that gelation is due to the hierarchical three-dimensional self-assembly of OPVs to form supramolecular tapes of high aspect ratio, assisted by π–π interactions and lamellar packing. The interesting feature of this system is the gelation-induced changes to the optical properties, particularly to the emission behavior, which is useful in probing the self-assembly and the sol–gel phenomena. The extent of modulation of the optical properties in three-dimensional self-assembly is remarkable when compared to that observed for one-dimensional aggregates, indicating strong electronic interaction of the chromophores within the self-assembled tapes. The three-dimensional growth of nanostructures, the gelation, and the consequent reversible changes in the optical properties assign these OPV organogels to a novel class of functional materials with tunable properties. This study should provide opportunities for the development of nanostructured advanced materials from the gelation of a variety of linear, π-conjugated systems and organic semiconductors, which may find applications in the emerging field of supramolecular electronics.

Acknowledgements

We are grateful to Prof. E. W. Meijer, Prof. R. A. J. Janssen, and Dr. A. P. H. J. Schenning of the Laboratory of Macromolecular and Organic Chemistry, Technology University of Eindhoven for their help and fruitful discussions. We thank Pascal Jonkheim and Jochaim de Loos of the Technology University of Eindhoven for the AFM and TEM measurements, respectively. The help of Mr. Gurusamy with XRD and Mr. Prabhakar Rao with SEM is gratefully acknowledged. This work was supported by the Department of Science and Technology (DST), Government of India, New Delhi and the CSIR Task Force program (CMM 010). S.J.G. thanks the CSIR for a research fellowship. This is manuscript No. RRL-PPD-194.

[1] a) J.-M. Lehn, *Supramolecular Chemistry*, VCH, Weinheim, **1995**; b) H.-J. Schneider, A. Yatsimirsky, *Principles and Methods in Supramolecular Chemistry*, Wiley, Chichester, **2000**; c) J. W. Steed, J. L. Atwood, *Supramolecular Chemistry*, Wiley, Chichester, **2000**.

[2] a) H. Engelkamp, S. Middelbeek, R. J. M. Nolte, *Science* **1999**, *284*, 785; b) R. Oda, I. Huc, M. Schmutz, S. J. Candau, F. C. MacKintosh, *Nature* **1999**, *399*, 566; c) L. J. Prins, J. Huskens, F. de Jong, P. Timmerman, D. N. Reinhoudt, *Nature* **1999**, *398*, 498; d) J. H. K. K. Hirschberg, L. Brunsveld, A. Ramzi, J. A. J. M. Vekemans, R. P. Sijbesma, E. W. Meijer, *Nature* **2000**, *407*, 167; e) V. Berl, I. Huc, R. G. Khoury, M. J. Krische, J.-M. Lehn, *Nature* **2000**, *407*, 720.

[3] a) J. C. Nelson, J. G. Saven, J. S. Moore, P. G. Wolynes, *Science* **1997**, *277*, 1793; b) J. S. Moore, *Acc. Chem. Res.* **1997**, *30*, 402; c) R. B. Prince, L. Brunsveld, E. W. Meijer, J. S. Moore, *Angew. Chem.* **2000**, *112*, 234; *Angew. Chem. Int. Ed.* **2000**, *39*, 228; d) L. Brunsveld, E. W. Meijer, R. B. Prince, J. S. Moore, *J. Am. Chem. Soc.* **2001**, *123*, 7978.

[4] a) D. T. Bong, T. D. Clark, J. R. Granja, M. R. Ghadiri, *Angew. Chem.* **2001**, *113*, 1016; *Angew. Chem. Int. Ed.* **2001**, *40*, 988 and the references cited therein; b) N. Sakai, S. Matile, *Chem. Commun.* **2003**, 2514 and the references cited therein.

[5] a) S. I. Stupp, V. LeBonheur, K. Walker, L. S. Li, K. E. Huggins, M. Keser, A. Amstutz, *Science* **1997**, *276*, 384; b) E. R. Zubarev, M. U. Pralle, L. Li, S. I. Stupp, *Science* **1999**, *283*, 523; c) J. D. Hartgerink, E. Beniash, S. I. Stupp, *Science* **2001**, *294*, 1684; d) E. R. Zubarev, M. U. Pralle, E. D. Sone, S. I. Stupp, *J. Am. Chem. Soc.* **2001**, *123*, 4105.

[6] a) F. Würthner, A. Sautter, D. Schmid, P. J. A. Weber, *Chem. Eur. J.* **2001**, *7*, 894; b) A. Sautter, D. G. Schmid, G. Jung, F. Würthner, *J. Am. Chem. Soc.* **2001**, *123*, 5424; c) L. J. Prins, C. Thalacker, F. Würthner, P. Timmerman, D. N. Reinhoudt, *Proc. Natl. Acad. Sci. USA* **2001**, *98*, 10042; d) F. Würthner, A. Sautter, *Org. Biomol. Chem.* **2003**, *1*, 240.

[7] a) J.-H. Fuhrhop, C. Demoulin, C. Boettcher, J. Koening, U. Siggel, *J. Am. Chem. Soc.* **1992**, *114*, 4159; b) H. A. M. Biemans, A. E. Rowan, A. Verhoeven, P. Vanoppen, L. Latterini, J. Foekema, A. P. H. J. Schenning, E. W. Meijer, F. C. De Schryver, R. J. M. Nolte, *J. Am. Chem. Soc.* **1998**, *120*, 11054; c) F. Würthner, C. Thalacker, A. Sautter, *Adv. Mater.* **1999**, *11*, 754; d) F. Würthner, C. Thalacker, A. Sautter, W. Schärtl, W. Ibach, O. Hollricher, *Chem. Eur. J.* **2000**, *6*, 3871; e) M. Kimura, T. Muto, H. Takimoto, K. Wada, K. Ohta, K. Hanabusa, H. Shirai, N. Kobayashi, *Langmuir* **2000**, *16*, 2078; f) T. Yamaguchi, N. Ishii, K. Tashiro, T. Aida, *J. Am. Chem. Soc.* **2003**, *125*, 13934; g) M. Kimura, T. Kuroda, K. Ohta, K. Hanabusa, H. Shirai, N. Kobayashi, *Langmuir* **2003**, *19*, 4825.

[8] a) D. T. McQuade, J. Kim, T. M. Swager, *J. Am. Chem. Soc.* **2000**, *122*, 5885; b) D. T. McQuade, A. H. Hegedus, T. M. Swager, *J. Am. Chem. Soc.* **2000**, *122*, 12389; c) U. H. F. Bunz, *Chem. Rev.* **2000**, *100*, 1605; d) U. H. F. Bunz, *Acc. Chem. Res.* **2001**, *34*, 998; e) M. Levitus, K. Schmieder, H. Ricks, K. D. Shimizu, U. H. F. Bunz, M. A. Garcia-Garibay, *J. Am. Chem. Soc.* **2001**, *123*, 4259; f) J. Kim, T. M. Swager, *Nature* **2001**, *411*, 1030; g) V. Percec, M. Glodde, T. K. Bera, Y. Miura, I. Shiyanovskaya, K. D. Singer, V. S. K. Balagurusamy, P. A. Heiney, I. Schnell, A. Rapp, H.-W. Spiess, S. D. Hudson, H. Duan, *Nature* **2002**, *417*, 384; h) L. Arnt, G. N. Tew, *J. Am. Chem. Soc.* **2002**, *124*, 7664; i) B. Liu, B. S. Gaylord, S. Wang, G. C. Bazan, *J. Am. Chem. Soc.* **2003**, *125*, 6705; j) R. B. Breitenkamp, G. N. Tew, *Macromolecules* **2004**, *37*, 1163.

[9] a) J.-F. Eckert, J.-F. Nicoud, D. Guillon, J.-F. Nierengarten, *Tetrahedron Lett.* **2000**, *41*, 6411; b) A. El-ghayoury, E. Peeters, A. P. H. J. Schenning, E. W. Meijer, *Chem. Commun.* **2000**, 1969; c) A. P. H. J. Schenning, P. Jonkheijm, E. Peeters, E. W. Meijer, *J. Am. Chem. Soc.* **2001**, *123*, 409; d) A. P. H. J. Schenning, J. van Herrikhuyzen, P. Jonkheijm, Z. Chen, F. Würthner, E. W. Meijer, *J. Am. Chem. Soc.* **2002**, *124*, 10252; e) P. Jonkheijm, F. J. M. Hoeben, R. Kleppinger, J. van Herrikhuyzen, A. P. H. J. Schenning, E. W. Meijer, *J. Am. Chem. Soc.* **2003**, *125*, 15941.

[10] For reviews on low molecular weight organogels, see: a) P. Terech, R. G. Weiss, *Chem. Rev.* **1997**, *97*, 3133; b) J. H. van Esch, B. L. Feringa, *Angew. Chem.* **2000**, *112*, 2351; *Angew. Chem. Int. Ed.* **2000**, *39*, 2263; c) K. J. C. van Bommel, A. Friggeri, S. Shinkai, *Angew. Chem.* **2003**, *115*, 1010; *Angew. Chem. Int. Ed.* **2003**, *42*, 980; d) L. A. Estorff, A. D. Hamilton, *Chem. Rev.* **2004**, *104*, 1201.

[11] a) A. Saiani, J.-M. Guenet, *Macromolecules* **1997**, *30*, 967; b) A. Saiani, J.-M. Guenet, *Macromolecules* **1999**, *32*, 657; c) U. Beginn, M. Möller, in *Supramolecular Materials and Technologies* (Ed.: D. N. Reinhoudt), Wiley, Chichester, **1999**, pp. 89–176.

[12] For cholesterol-based organogels, see: a) Y. C. Lin, B. Kachar, R. G. Weiss, *J. Am. Chem. Soc.* **1989**, *111*, 5542; b) K. Murata, M. Aoki, T. Suzuki, T. Harada, H. Kawabata, T. Komori, F. Ohseto, K. Ueda, S. Shinkai, *J. Am. Chem. Soc.* **1994**, *116*, 6664; c) E. Ostuni, P. Kamaras, R. G. Weiss, *Angew. Chem.* **1996**, *108*, 1423; *Angew. Chem. Int. Ed. Engl.* **1996**, *35*, 1324; d) J. H. Jung, Y. Ono, S. Shinkai, *Angew. Chem.* **2000**, *112*, 1931; *Angew. Chem. Int. Ed.* **2000**, *39*, 1862; e) J. H. Jung, H. Kobayashi, M. Masuda, T. Shimizu, S. Shinkai, *J. Am. Chem. Soc.* **2001**, *123*, 8785; f) R. Wang, C. Geiger, L. Chen, B. Swanson, D. G. Whitten, *J. Am. Chem. Soc.* **2000**, *122*, 2399.

[13] For urea-derived organogels, see: a) K. Hanabusa, K. Shimura, K. Hirose, M. Kimura, H. Shirai, *Chem. Lett.* **1996**, 885; b) J. van Esch, R. M. Kellogg, B. L. Feringa, *Tetrahedron Lett.* **1997**, *38*, 281; c) M. de Loos, J. van Esch, I. Stokroos, R. M. Kellogg, B. L. Feringa, *J. Am. Chem. Soc.* **1997**, *119*, 12675; d) J. van Esch, F. Schoonbeek, M. de Loos, H. Kooijman, A. L. Spek, R. M. Kellogg, B. L. Feringa, *Chem. Eur. J.* **1999**, *5*, 937; e) L. A. Estroff, A. D. Hamilton, *Angew. Chem.* **2000**, *112*, 3589; *Angew. Chem. Int. Ed.* **2000**, *39*, 3447; f) M. de Loos, J. van Esch, R. M. Kellogg, B. L. Feringa, *Angew. Chem.* **2001**, *113*, 633; *Angew. Chem. Int. Ed.* **2001**, *40*, 613; g) J. J. van-Gorp, J. A. J. M. Vekemans, E. W. Meijer, *J. Am. Chem. Soc.* **2002**, *124*, 14759.

[14] For amide-based organogels, see: a) K. Hanabusa, Y. Matsumoto, T. Miki, T. Koyama, H. Shirai, *J. Chem. Soc. Chem. Commun.* **1994**, 1401; b) K. Hanabusa, M. Yamada, M. Kimura, H. Shirai, *Angew. Chem.* **1996**, *108*, 2086; *Angew. Chem. Int. Ed. Engl.* **1996**, *35*, 1949; c) J. E.-S. Sohana, F. Fages, *Chem. Commun.* **1997**, 327.

[15] For sugar-based gels, see: a) R. J. H. Hafkamp, M. C. Feiters, R. J. M. Nolte, *J. Org. Chem.* **1999**, *64*, 412; b) K. Yoza, N. Amanokura, Y. Ono, T. Akao, H. Shinmori, M. Takeuchi, S. Shinkai, D. N. Reinhoudt, *Chem. Eur. J.* **1999**, *5*, 2722; c) G. John, M. Masuda, Y. Okada, K. Yase, T. Shimizu, *Adv. Mater.* **2001**, *13*, 715; d) O. Gronwald, S. Shinkai, *Chem. Eur. J.* **2001**, *7*, 4329; e) J. H. Jung, G. John, M. Masuda, K. Yoshida, S. Shinkai, T. Shimizu, *Langmuir* **2001**, *17*, 7229; f) G. John, J. H. Jung, H. Minamikawa, K. Yoshida, T. Shimizu, *Chem. Eur. J.* **2002**, *8*, 5494; g) J. H. Jung, S. Shinkai, T. Shimizu, *Chem. Eur. J.* **2002**, *8*, 2684; h) H. Kobayashi, A. Friggeri, K. Koumoto, M. Amaike, S. Shinkai, D. N. Reinhoudt, *Org. Lett.* **2002**, *4*, 1423.

[16] For amino acid-derived organogels, see: a) S. Bhattacharya, S. N. G. Acharya, *Chem. Mater.* **1999**, *11*, 3121; b) F. M. Menger, K. L. Caran, *J. Am. Chem. Soc.* **2000**, *122*, 11679; c) K. Hanabusa, M. Matsumoto, M. Kimura, A. Kakehi, H. Shirai, *J. Colloid Interface Sci.* **2000**, *224*, 231; d) G. Mieden-Gundert, L. Klein, M. Fischer, F. Vögtle, K. Heuzé, J.-L. Pozzo, M. Vallier, F. Fages, *Angew. Chem.* **2001**, *113*, 3266; *Angew. Chem. Int. Ed.* **2001**, *40*, 3164; e) M. Suzuki, M. Yumoto, M. Kimura, H. Shirai, K. Hanabusa, *Chem. Commun.* **2002**, 884; f) L. Frkanec, M. Jokić, J. Makarević, K. Wolsperger, M. Žinić, *J. Am. Chem. Soc.* **2002**, *124*, 9716; g) G. Wang, A. D. Hamilton, *Chem. Eur. J.* **2002**, *8*, 1954.

[17] For miscallaneous gels, see: a) U. Maitra, P. V. Kumar, N. Chandra, L. J. D'Souza, M. D. Prasanna, A. R. Raju, *Chem. Commun.* **1999**, 595; b) A. Friggeri, O. Gronwald, K. J. C. van Bommel, S. Shinkai, D. N. Reinhoudt, *J. Am. Chem. Soc.* **2002**, *124*, 10754; c) M. George, R. G. Weiss, *J. Am. Chem. Soc.* **2001**, *123*, 10393; d) M. George, R. G. Weiss, *Langmuir* **2003**, *19*, 1017; e) R. Oda, I. Huc, S. J. Candau, *Angew. Chem.* **1998**, *110*, 2835; *Angew. Chem. Int. Ed.* **1998**, *37*, 2689; f) S. Yagai, M. Higashi, T. Karatsu, A. Kitamura, *Chem. Mater.* **2004**, *16*, 3582.

[18] For miscellaneous, chromophore-derived organogels, see: a) T. Brotin, R. Utermöhlen, F. Fages, H. Bouas-Laurent, J.-P. Desvergne, *J. Chem. Soc. Chem. Commun.* **1991**, 416; b) G. M. Clavier, J.-F. Brugger, H. Bouas-Laurent, J.-L. Pozzo, *J. Chem. Soc. Perkin Trans. 2* **1998**, 2527; c) T. Nakashima, N. Kimizuka, *Adv. Mater.* **2002**, *14*, 1113; d) M. Shirakawa, S. Kawano, N. Fujita, K. Sada, S. Shinkai, *J. Org. Chem.* **2003**, *68*, 5037; e) K. Sugiyasu, N. Fujita, M. Takeuchi, S. Yamada, S. Shinkai, *Org. Biomol. Chem.* **2003**, *1*, 895; f) M. Shirakawa, N. Fujita, S. Shinkai, *J. Am. Chem. Soc.* **2003**, *125*, 9902; g) M. Ikeda, M. Takeuchi, S. Shinkai, *Chem. Commun.* **2003**, 1354; h) F. Würthner, S. Yao, U. Beginn, *Angew. Chem.* **2003**, *115*, 3368; *Angew. Chem. Int. Ed.* **2003**, *42*, 3247; i) S. Yagai, T. Karatsu, A. Kitamura, *Chem. Commun.* **2003**, 1844; j) S. Yao, U. Beginn, T. Gress, M. Lysetska, F. Würthner, *J. Am. Chem. Soc.* **2004**, *126*, 8336; k) J. J. D. de Jong, L. N. Lucas, R. M. Kellog, J. H. van Esch, B. L. Feringa, *Science* **2004**, *304*, 278; l) K. Sugiyasu, N. Fujita, S. Shinkai, *Angew. Chem.* **2004**, *116*, 1249; *Angew. Chem. Int. Ed.* **2004**, *43*, 1229; m) R. Zeissel, G. Pickaert, F. Camerel, B. Donnio, D. Gullion, M. Cesario, T. Prangé, *J. Am. Chem. Soc.* **2004**, *126*, 12403.

[19] a) F. S. Schoonbeek, J. H. van Esch, B. Wegewijs, D. B. A. Rep, M. P. de Haas, T. M. Klapwijk, R. M. Kellogg, B. L. Feringa, *Angew. Chem.* **1999**, *111*, 1486; *Angew. Chem. Int. Ed.* **1999**, *38*, 1393; b) N. Tamaoki, S. Shimada, Y. Okada, A. Belaissaoui, G. Kruk, K. Yase, H. Matsuda, *Langmuir* **2000**, *16*, 7545; c) C.-H. Lin, J. Tour, *J. Org. Chem.* **2002**, *67*, 7761; d) M. George, R. G. Weiss, *Chem. Mater.* **2003**, *15*, 2879; e) N. Koumura, M. Kudo, N. Tamaoki, *Langmuir* **2004**, *20*, 9897; f) B.-K. An, D.-S. Lee, J.-S. Lee, Y.-S. Park, H.-S. Song, S. Y. Park, *J. Am. Chem. Soc.* **2004**, *126*, 10232.

[20] a) A. Ajayaghosh, S. J. George, *J. Am. Chem. Soc.* **2001**, *123*, 5148; b) A. Ajayaghosh, S. J. George, V. K. Praveen, *Angew. Chem.* **2003**, *115*, 346; *Angew. Chem. Int. Ed.* **2003**, *42*, 332; c) S. J. George, A. Ajayaghosh, P. Jonkheijm, A. P. H. J. Schenning, E. W. Meijer, *Angew. Chem.* **2004**, *116*, 3504; *Angew. Chem. Int. Ed.* **2004**, *43*, 3421.

[21] During the preparation of this manuscript, Stupp and co-workers reported the formation of supramolecular polymeric ribbons and the gelation of dendron rodcoil molecules that contain conjugated segments. For details, see: B. W. Messmore, J. F. Hulvat, E. D. Sone, S. I. Stupp, *J. Am. Chem. Soc.* **2004**, *126*, 14452.

[22] B. Wang, M. R. Wasielewski, *J. Am. Chem. Soc.* **1997**, *119*, 12.

[23] S.-A. Chen, E.-C. Chang, *Macromolecules* **1998**, *31*, 4889.

[24] R. Luboradzki, O. Gronwald, A. Ikeda, S. Shinkai, *Chem. Lett.* **2000**, 1148.

Received: November 19, 2004
Published online: February 25, 2005

